

NIH RELAIS Document Delivery

NIH-10286724

JEFFDUYN

NIH -- W1 MA34IF

JOZEF DUYN
10 Center Dirve
Bldg. 10/Rm.1L07
Bethesda, MD 20892-1150

ATTN: SUBMITTED: 2002-08-29 17:22:18
PHONE: 301-594-7305 PRINTED: 2002-09-03 07:36:35
FAX: - REQUEST NO.: NIH-10286724
E-MAIL: SENT VIA: LOAN DOC
7967425

NIH	Fiche to Paper	Journal
TITLE:	MAGNETIC RESONANCE IN MEDICINE : OFFICIAL JOURNAL OF THE SOCIETY OF MAGNETIC RESONANCE IN MEDICINE / SOCIETY OF MAGNETIC RESONANCE IN MEDICINE	
PUBLISHER/PLACE:	Wiley-Liss, Inc., a division of John Wil New York, NY :	
VOLUME/ISSUE/PAGES:	1994 Jul;32(1):150-5 150-5	
DATE:	1994	
AUTHOR OF ARTICLE:	Duyn JH; Mattay VS; Sexton RH; Sobering GS; Barrios FA; Liu	
TITLE OF ARTICLE:	3-dimensional functional imaging of human brain us	
ISSN:	0740-3194	
OTHER NOS/LETTERS:	Library reports holding volume or year 8505245 8084232	
SOURCE:	PubMed	
CALL NUMBER:	W1 MA34IF	
REQUESTER INFO:	JEFFDUYN	
DELIVERY:	E-mail: jhd@helix.nih.gov	
REPLY:	Mail:	

NOTICE: THIS MATERIAL MAY BE PROTECTED BY COPYRIGHT LAW (TITLE 17, U.S. CODE)

---National-Institutes-of-Health,-Bethesda,-MD-----

3-Dimensional Functional Imaging of Human Brain Using Echo-Shifted FLASH MRI

Jeff H. Duyn, Venhatha S. Mattay, Roy H. Sexton, Geoffrey S. Sobering, Fernando A. Barrios, Guoying Liu, Joseph A. Frank, Daniel R. Weinberger, Chrit T. W. Moonen

A 3-dimensional MRI method has been developed for functional mapping of the human brain, based on blood oxygenation level dependent (BOLD) contrast mechanisms. The method uses recently introduced principles of echo-shifted FLASH to acquire a single 3D data set in 20 s. The technique was tested on a conventional 1.5 Tesla clinical scanner with a standard head coil using visual stimulation with a 8 Hz flashing white light, or a varying checkerboard pattern. Areas of increased signal intensity were identified in the visual cortex, consistent with the known functional organization.

Key words: brain, function; brain, MR; MR, rapid imaging; functional MRI.

INTRODUCTION

The prospect of mapping the functional organization of human brain without the use of exogenous contrast agents has gained increased interest since the introduction of MR functional imaging based on blood oxygenation level dependent (BOLD) contrast mechanisms (1, 2). Most MR functional imaging methods use echo-planar (EPI) or fast gradient-echo (FLASH) techniques, and repetitively scan a single slice (2D) through the brain during execution of a specific stimulation paradigm (3–14). Activation induced changes in deoxyhemoglobin levels result in changes in microscopic susceptibility effects and are measured as small increases in image intensity. The magnitude of these BOLD-related signal increases are reportedly on the order of 1–3% at 1.5 T and increase with field strength (6).

When repeatedly exciting a single slice using a short repetition time and large flip angle, unsaturated water, flowing into the observed slice from neighboring regions, may represent a large fraction of the signal intensity. This sensitivity to “in-flow” may also lead to signal changes upon activation when, for example, the flow velocity increases in a vein draining an activated brain region. It was recently shown that the in-flow effect may dominate the BOLD effect in gradient echoes under certain experi-

mental conditions (15, 16). The inflow effect may include venous and arterial water, and even CSF, and should thus be differentiated from “perfusion” effects when the magnetization of arterial water only is altered, as described by Detre *et al.* (17). Despite the success of several functional 2D MRI studies in identifying the approximate location of activated brain regions, many studies now suggest that large vessels may play an important role, whether the predominant effect is a true “BOLD” phenomenon or an “in-flow” phenomenon (15, 16, 18–23).

Since, in many cases, the area of cortical activation during sensory, memory, motor, or cognitive activation is not always *a priori* known, nor is it necessarily confined to a single slice, the desire has grown to observe multiple slices simultaneously. Multislice methods would allow mapping of large parts of the brain. However, interpretation is complicated by in-flow effects because water excited during scanning of plane *i* may give rise to signal changes in plane *j* upon flow from *i* to *j* within the T_1 relaxation time. Simple extension of existing 2D techniques to true 3D versions would limit in-flow effects but severely restrict the in-plane resolution, due to inherent limitations on the acquisition time per excitation (in the case of single shot volume acquisition) or the limited total acquisition time (in the case of FLASH). Most recently, echo-shifted (ES)-FLASH was introduced (24–26), reducing the total acquisition time, and allowing the extension toward full 3D functional imaging. Here, we will discuss a particular implementation of 3D ES-FLASH for functional imaging on a standard clinical scanner with a conventional head coil. Preliminary results have been presented previously (27).

METHODS

All studies ($n = 13$) were performed on a 1.5 T GE/SIGNA scanner (General Electric, Milwaukee, WI) using the standard GE quadrature head coil. The patient protocol was approved by the intramural review board of the National Institute of Mental Health.

The 3D ES-FLASH pulse sequence (Fig. 1) was based on its 2D counterpart (24–26), and had additional phase encoding in the slice select direction. For improved suppression of unwanted coherences, additional gradient crushers of 3 ms duration in both phase encode directions before and after the data acquisition period were used. These crushers were of -0.3 G/cm and 0.6 G/cm strength, respectively, resulting in selection of a single TR -shifted gradient echo. Note that the additional gradients remain identical in all TR periods. The additional gradient prior to the acquisition period serves to dephase

MRM 32:150–155 (1994)

From the Laboratory of Diagnostic Radiology Research, OIR, NIH, Bethesda, Maryland (J.H.D., V.S.M., J.A.F.); NIH In Vivo NMR Research Center, BEIP, NCI, National Institutes of Health, Bethesda, Maryland (J.H.D., G.S.S., G.L., C.T.W.M.); Clinical Brain Disorders Branch, NIMH, NIH, Washington, DC (R.H.S., F.A.B., D.R.W.); and Computational Physics, Inc., Fairfax, Virginia (F.A.B.).

Address correspondence to: Chrit T. Moonen, Ph.D., In Vivo NMR Research Center, BEIP, NCI, National Institutes of Health, Building 10, Room 1D-125, Bethesda, MD 20892.

Received October 26, 1993; revised March 22, 1994; accepted April 1, 1994.

0740-3194/94 \$3.00

Copyright © 1994 by Williams & Wilkins

All rights of reproduction in any form reserved.

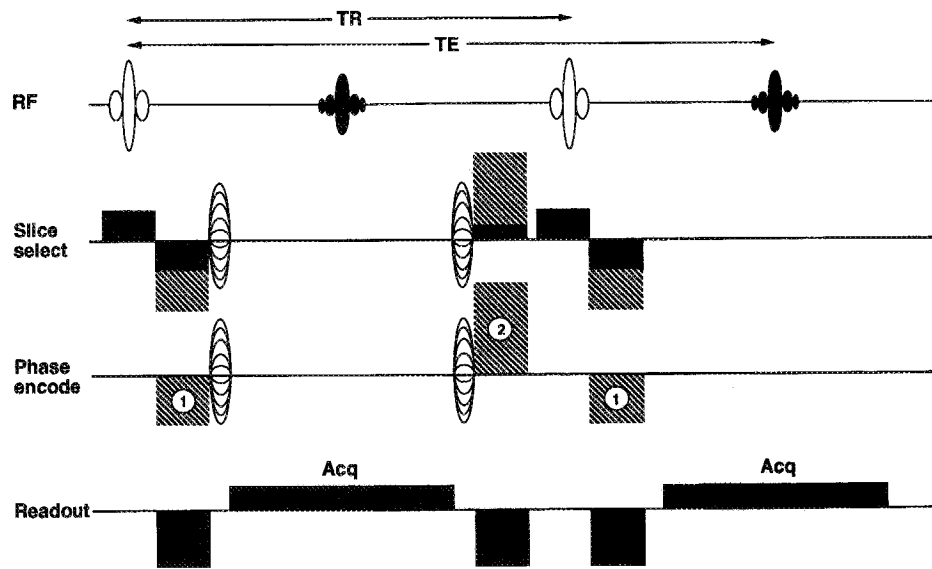


FIG. 1. Pulse sequence for 3D ES-FLASH. Gradient waveforms in black result in rephasing of the shifted echo in the subsequent TR-period and have been described previously (24–26). The hatched waveforms are additional gradients which serve to dephase unwanted gradient and spin echoes. The relative surface area of the negative additional lobe prior to the acquisition period relative to that after the data acquisition is 1:2.

unwanted gradient echoes, whereas the gradient crusher after the acquisition period serves to dephase stimulated and spin echoes. See ref. 25 for the extent of attenuation of unwanted coherences in ES-FLASH by gradient crushers. The use of strong crushers in this study (as compared with the ES-FLASH method for bolus tracking reported in ref. 26) was based on the anticipated small BOLD effect and thus the increased demand on the attenuation of unwanted coherences. In addition, RF spoiling was used to achieve coherent phase between RF and receiver for the shifted echo and incoherent phase for all other signals. A 20 ms/30 ms TR/TE combination was used. A 4-cm thick angulated slab was selected with the calcarine fissure in the center of the slab. A data matrix of $64 \times 64 \times 16$ was used in combination with a $24 \times 24 \times 6.4$ cm FOV. This resulted in 16 slices of 4 mm width, of which only the central 10 were used. The sampling frequency was 8 kHz, and the total acquisition time for a 3D data set was 20 s. An RF flip angle of 6–12° was used. This was below the calculated ERNST angle for gray matter (13° assuming $T_1 = 800$ ms), resulting in reduced spin saturation and thus reduced in-flow sensitivity. In a single study, residual inflow effects were assessed by varying the pulse angle between 6°, 12°, and 24°.

For comparison, single-slice gradient-echo functional MRI was also performed on all subjects using conventional methods and parameters as described recently (9, 10, 11, 13): flip angle = 40°, TE = 38 ms, TR = 60 ms, slice thickness = 4 mm, and a location corresponding to one of the center slices of the 3D volume studied with 3D ES-FLASH. A 128×128 data matrix was used over a 24×24 cm FOV. A 20% Hamming filter was used for data processing.

Visual stimulation paradigms were used consisting of eight stages, alternating rest (dark) stages and stages with stimulus. Two types of stimuli were used: a flashing light (8 Hz frequency) ($n = 9$) or a varying (8 Hz) checkerboard pattern ($n = 4$). Although both types of visual stimulation may lead to different activation, we concentrated on the V1 part of the visual cortex which is known to be activated extensively upon both types of stimulation. Each

activation study was preceded by a 4-s period in which no data were collected, in order to reach a steady-state. The total measurement time amounted to 2.6 min. Anatomical scout images were recorded after each study using conventional spin echo sequences for proper, anatomy based, selection of the primary visual cortex.

Data were processed off-line on Sun-SPARC workstations (Sun Microsystems, Mountainview, CA) using IDL processing software (Research Systems, Boulder, CO). For each activation study, the eight 3D data sets recorded during the stimulation protocol were apodized using 20% Hamming filters in all three directions and subsequently Fourier transformed. Actual image resolution is approximately $4.5 \times 4.5 \times 4.8$ mm. First, a correlation image was created by cross-correlating the time course of the image intensity with the time course of the stimulation as described previously (28, 29). The reference vector was a boxcar function, with a phase identical to that of the activation timing. A correlation level of 0.6 was then used as a threshold to define pixels for the difference image. The cut-off level is chosen on the proper filtering of the majority of white noise voxels outside the brain. The particular correlation threshold reflects the maximum signal difference between on/off states, and the number of data points in the time series. Then, for each slice, a correlation thresholded difference image was created by subtracting the sum of the "baseline" images (images recorded during a rest stage) from the sum of the "activated" images (images recorded during stimulus stage) masked by the correlation threshold of 0.6.

In order to quantify percentage signal changes and to evaluate specificity of our method, all studies were analyzed in the following way. First, the center two slices of each study were selected. In each slice, three different anatomical regions of interest (ROIs) were chosen: two ROIs covering the larger part of the visual cortex (30), i.e., one in the left and the other one in the right hemisphere. Because of the tortuosity of calcarine fissure we estimate that at least 50% of these ROIs is taken up by the primary visual cortex. A third ROI was chosen as a control, in a fronto-parietal area of no suspected sensory or cognitive

relevance. All ROIs were of similar size and included approximately 2.5 ml tissue consisting of predominantly gray matter. Then, the correlation thresholded difference images were studied in each ROI, and the percentage area above threshold was determined, as well as the average signal increase in the ROI voxels above threshold. Finally, the results were averaged over the two selected slices of each study.

RESULTS AND DISCUSSION

All activation studies resulted in 3D data sets with good SNR and no significant artifacts. Image SNR for gray matter varied between 80 and 120 for the center slices of the 3D images. The use of the additional crusher gradients in both slice-select and phase-encode directions resulted in improved signal stability in the images. We attribute this in part to the improved suppression of unwanted signal from spin echoes and unwanted gradient echoes. In 10 of the 13 studies performed, the stability (intensity variation over time) for single gray matter pixels in the rest images was within $\pm 1.5\%$. Activation of the primary visual cortex could be easily identified in all these studies (see below). The remaining three studies showed excessive instability (2–5%), did not show clear activation patterns, and were labeled as unsuccessful.

Figure 2a shows an example from a study using checkerboard stimulation. "Baseline" echo-shifted FLASH images of six slices are displayed, encompassing the calcarine fissure. The 3D ES-FLASH images show considerable anatomical detail. Correlation thresholded difference images (see Methods) are overlaid in color. Largest percentage differences were found in the primary visual cortex. Because of the 3D acquisition mode, images can be reformatted for any desired orientation. Figure 2b contains a series of reformatted sagittal images with the highest percentage difference found along the calcarine fissure. The 10 successful studies resulted in activation images of similar quality with respect to SNR and amount of pixels identified as "activated."

A slightly different activation pattern was observed depending on the type of visual stimulation. For flashing light stimulation the activated area was generally larger than for checkerboard stimulation. However, ROIs for further quantitative analysis were chosen only from the primary visual cortex as previously reported (30). These ROIs were further analyzed regardless of whether stimulation with checkerboard or flashing lights was used. The results of the 10 studies with adequate stability are summarized in Table 1. Note that a large area (27%) within the visual cortex ROIs is identified as "activated" (correlation coefficient ≥ 0.6). The average signal difference is of the order of 2.5%. For comparison, the ROI chosen in the fronto/parietal region showed a much smaller (and inconsistent among subjects) area identified with a correlation coefficient ≥ 0.6 . The percent change in these pixels was 1.0%. However, by selecting only those pixels with a positive correlation coefficient, a bias is introduced leading to a positive intensity change for these pixels. We have explored this further by simulating the influence of this correlation bias with white noise gener-

ated within $\pm 1.5\%$ of maximum amplitude. Using a correlation threshold of 0.6, a 1.1% change was found for these thresholded pixels. Therefore, the change of 1.0% in the fronto/parietal region is probably the result of the correlation bias and is not due to an "activation" effect.

The 3D-ES-FLASH method is rather insensitive to in-flow effects, especially with respect to the middle slices of the slab. However, in-flow effects cannot be fully excluded. The studies performed with a varying flip angle using checkerboard stimulation showed very similar "activation" patterns. Signal increases in anatomically selected ROIs from visual cortex were 3.1%, 3.1%, and 4.2% for flip angles of 6° , 12° , and 24° respectively, suggesting only minor influence of in-flow in the 3D method at the lower flip angles.

These results confirm that the 3D BOLD-type functional imaging method based on echo-shifting principles allows the evaluation of activated regions in a simple visual stimulation paradigm using a conventional MR instrument and a standard head coil. Difference images showed that the signal increases in the "hottest" pixels amount to 2–5% of the value during the dark condition. This increase corresponds well with previous results using EPI techniques at 1.5 T. However, conventional 2D gradient echo techniques at 1.5 or 2.0 T have been reported to show larger signal changes upon stimulation. At field strengths of 1.5 T and 2.0 T, signal increases varying between 1% and 40% have been reported (9, 10, 11, 13), depending on technique and experimental parameters. In a previous study, we have shown that "in-flow" effects may dominate the signal changes upon activation when using a conventional 2D gradient echo technique with large flip angle (15). To compare activation maps from the 3D-ES-FLASH and conventional 2D gradient echo imaging we included activation experiments using the latter technique in all our studies. An example of the results is shown in Fig. 3. Note that the 2D FLASH and 3D ES-FLASH results were obtained with different *TE* and *TR* values, and with a different resolution. Therefore, a quantitative comparison cannot be performed. On a qualitative level, it can be seen that the 2D difference image, and the image of the corresponding slice from the 3D data set show similar locations of "activated" areas, although some distinct differences are observed. For example, the 2D activation map shows a few "hot" pixels in the visual cortex but shows a slightly different part of the visual cortex "activated" as compared with the corresponding slice from the 3D map. In this subject, the hottest pixels in the 2D image showed signal changes of up to 20%. Similar results were obtained in all volunteers (22). These results show that similar, although not identical, maps may be obtained with both methods despite the possibly different underlying physiological effects. Note that the 2D technique is rather similar to a 2D time-of-flight MR angiographic sequence and is sensitive to in-flow, in particular when using flip angles larger than the Ernst angle.

Several studies suggest that functional MR imaging based on 2D FLASH methods may show predominantly draining vessels (15, 16, 18–23). Although the 3D-ES-FLASH studies suggest a predominant BOLD effect, this

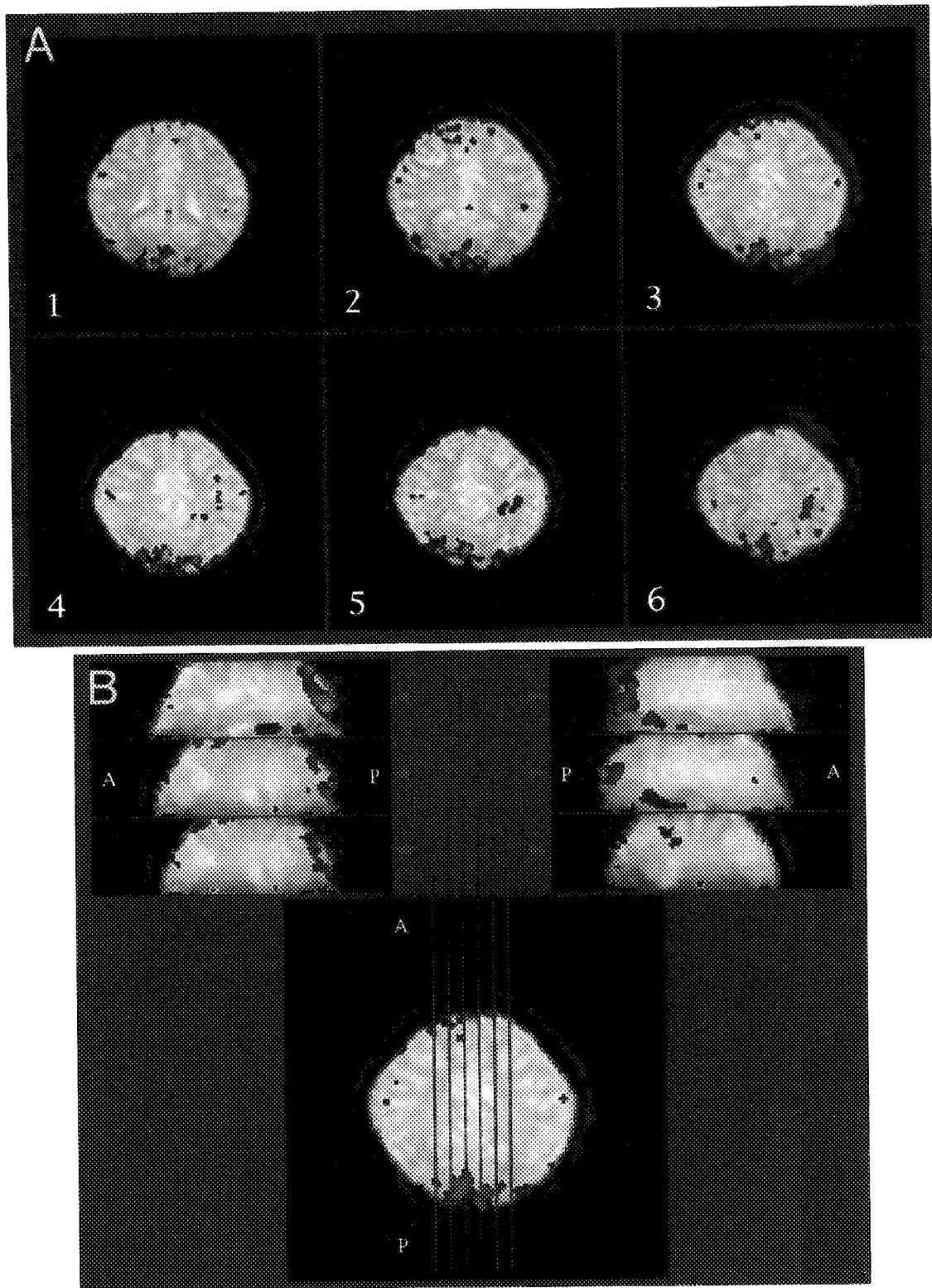


FIG. 2. 3D ES-FLASH functional MRI using checkerboard visual stimulation. Difference images were created masked with a correlation threshold of 0.6 (see text), and are superimposed in color on a dataset acquired during a "dark" stage. The color scale from red to yellow corresponds with differences of +2% to +4%. The blue color indicates a negative difference. (a) Six axial slices (top is anterior) selected from the central part of the 16-slice data set. Signal increases are observed posterior, corresponding with the primary visual cortex. (b) Six reformatted sagittal slices, calculated from the 16 axial slices. Locations are indicated with the vertical lines in the axial image (bottom). Anterior and posterior sides are indicated with a and p, respectively.

Table 1
Signal Increases upon Stimulation in Three Different ROIs

	Left vc	Right vc	Fronto/parietal
Area (%)	27	27	6
% Increase (SD)	2.6 (1.0)	2.5 (0.9)	1.1 (0.6)

The first row gives the percentage pixels (area) in each ROI with a correlation coefficient above 0.6. Signal increases (second row) were calculated from these pixels, and subsequently averaged over all subjects ($n = 10$) with the standard deviation (SD) calculated for the 10 successful studies.

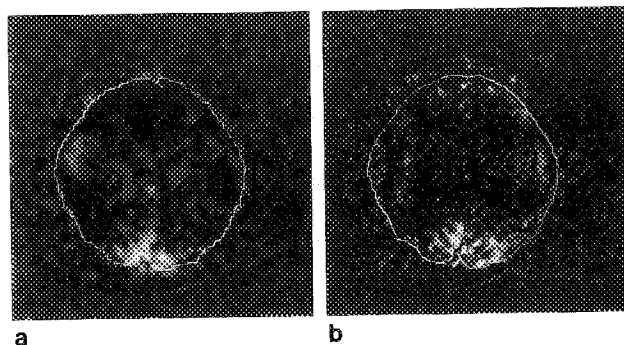


FIG. 3. Qualitative comparison between (a) 3D ES-FLASH, and (b) 2D FLASH functional MRI results for an identical brain slice shown as difference images (light minus dark). All results were obtained in a single study using a checkerboard visual stimulation paradigm. The outline of the brain is indicated for reference. (a) Single slice out of a 3D ES-FLASH dataset. (b) Corresponding single slice (difference image) obtained with 2D FLASH. Note the differences in acquisition parameters; flip angle (a) 12, (b) 40; resolution (a) 64×64 , (b) 128×128 ; signal-to-noise ratio (a) 100, (b) 30.

effect may not necessarily arise only from the capillary network, but may also involve the effect of larger vessels.

For BOLD-type functional MRI at 1.5 Tesla, particular attention must be paid to signal stability due to the small signal changes expected upon stimulation. The purpose of the additional gradient crushers is to reduce artifacts by attenuating unwanted coherences and selecting only the shifted gradient echo (24, 25). This is of particular importance for CSF which otherwise adds to signal instability due to its macroscopic flow in combination with the long T_1 , T_2 , and T_2^* . We tentatively attribute the three unsuccessful 3D ES-FLASH studies to remaining instabilities.

CONCLUSION

A fast 3D functional MRI method has been developed for use on conventional 1.5 T clinical scanners with a standard head coil. The stability was sufficient to detect small signal changes in the visual cortex upon activation by photic stimulation.

ACKNOWLEDGMENTS

The authors thank Jeannette Black, René Hill, and Susan Inscoc for technical assistance.

This work was performed in the In Vivo NMR Research Center at the NIH.

REFERENCES

1. S. Ogawa, T. M. Lee, A. S. Nayak, P. Glynn, Oxygenation-sensitive contrast in magnetic resonance imaging of rodent brain at high magnetic fields. *Magn. Reson. Med.* **14**, 68–78 (1990).
2. S. Ogawa, T. M. Lee, A. R. Ray, D. W. Tank, Brain magnetic resonance imaging with contrast dependent on blood oxygenation. *Proc. Natl. Acad. Sci. (USA)* **87**, 9868–9872 (1990).
3. R. Turner, D. LeBihan, C. T. W. Moonen, D. Despres, J. A. Frank, Echo-planar time course MRI of cat brain oxygenation. *Magn. Reson. Med.* **22**, 159–199 (1991).
4. K. K. Kwong, J. W. Belliveau, D. A. Chesler, I. E. Goldberg, R. M. Weiskoff, B. P. Poncelet, D. N. Kennedy, B. E. Hoppel, M. S. Cohen, R. Turner, H. Cheng, T. J. Brady, B. R. Rosen, Dynamic magnetic resonance imaging of human brain activity during primary sensory stimulation. *Proc. Natl. Acad. Sci. (USA)* **89**, 5675–5679 (1992).
5. S. Ogawa, D. W. Tank, R. Menon, J. M. Ellerman, S. Kim, H. Merkle, K. Ugurbil, Intrinsic signal changes accompanying sensory stimulation: functional brain mapping using MRI. *Proc. Natl. Acad. Sci. (USA)* **89**, 5951–5955 (1992).
6. R. Turner, P. Jezzard, H. Wen, K. K. Kwong, D. LeBihan, T. Zeffiro, B. Balaban, Functional mapping of the human visual cortex at 4 and 1.5 Tesla using deoxygenation contrast EPI. *Magn. Reson. Med.* **29**, 277–279 (1993).
7. P. A. Bandettini, E. C. Wong, R. S. Hinks, R. S. Tikofsky, J. S. Hyde, Time course EPI of human brain function during task activation. *Magn. Reson. Med.* **25**, 390–397 (1992).
8. A. M. Blamire, S. Ogawa, K. Ugurbil, D. Rothman, G. McCarthy, J. M. Ellerman, F. Hyder, Z. Rattner, R. S. Shulman, Dynamic mapping of the human visual cortex by high speed magnetic resonance imaging. *Proc. Natl. Acad. Sci. (USA)* **89**, 11069–11073 (1992).
9. J. Frahm, H. Bruhn, K. Merboldt, W. Hänicke, Dynamic MR imaging of human brain oxygenation during rest and photic stimulation. *J. Magn. Reson. Imaging* **2**, 501–505 (1992).
10. J. Frahm, K. Merboldt, W. Hänicke, Functional MRI of human brain activation at high spatial resolution. *Magn. Reson. Med.* **29**, 139–144 (1993).
11. A. Connelly, G. D. Jackson, R. S. J. Frackowiak, J. W. Belliveau, F. Vargha-Khadem, D. G. Gadian, Functional mapping of activated human primary cortex with a clinical MR imaging system. *Radiology* **188**, 125–130 (1993).
12. R. S. Menon, S. Ogawa, D. W. Tank, K. Ugurbil, 4 Tesla gradient recalled echo characteristics of photic stimulation-induced signal changes in the human primary visual cortex. *Magn. Reson. Med.* **30**, 380–386 (1993).
13. S. G. Kim, J. Ashe, K. Hendrich, J. M. Ellermann, H. Merkle, K. Ugurbil, A. P. Georgopoulos, Functional magnetic resonance imaging of motor cortex: hemispheric asymmetry and handedness. *Science* **261**, 615–617 (1993).
14. W. Schneider, D. C. Noll, J. D. Cohen, Functional topographic mapping of the cortical ribbon in human vision with conventional MRI scanners. *Nature* **365**, 150–153 (1993).
15. J. H. Duyn, C. T. W. Moonen, R. W. de Boer, G. H. van Yperen, P. R. Luyten, Inflow versus deoxyhemoglobin effects in “BOLD” functional MRI using gradient echoes at 1.5T. *NMR Biomed.* **7**, 83–88 (1994).
16. J. V. Hajnal, S. J. White, J. M. Pennock, A. Oatridge, C. J. Baudoin, I. R. Young, G. M. Bydder, Functional imaging of the brain at 1.0 and 0.15 T using fluid attenuated inversion recovery (FLAIR) pulse sequences, in “Proc., SMRM, 11th Annual Meeting, 1992,” p. 1023.
17. J. A. Detre, J. S. Leigh, D. S. Williams, A. P. Koretsky, Perfusion imaging. *Magn. Reson. Med.* **23**, 37–45, (1992).

18. J. V. Hajnal, A. Oatridge, J. Schwieso, F. M. Cowan, I. R. Young, G. M. Bydder, Cautionary remarks on the role of veins in the variability of functional imaging experiments, in "Proc., SMRM, 12th Annual Meeting, 1993," p. 166.
19. Z. H. Cho, Y. M. Ro, J. B. Park, S. C. Chung, S. H. Park, Functional brain imaging using blood flow changes, in "Proc., SMRM, 12th Annual Meeting, 1993," p. 170.
20. G. H. van Yperen, R. W. de Boer, J. W. Berkelbach van der Sprenkel, J. Verheul, P. R. Luyten, TSE and increased perfusion during activation of the motor cortex, in "Proc., SMRM, 12th Annual Meeting, 1993," p. 171.
21. K. K. Kwong, D. A. Chesler, C. S. Zuo, J. L. Boxerman, J. R. Baker, Y. C. Chen, C. E. Stern, R. M. Weiskoff, B. R. Rosen, Spin echo (T_2 , T_1) studies for functional MRI, in "Proc., SMRM, 12th Annual Meeting, 1993," p. 172.
22. S. Lai, A. Hopkins, E. M. Haacke, D. Li, B. Wasserman, P. Buckley, L. Friedman, H. Meltzer, P. Hedera, R. Friedland, Identification of vascular structures as a major source of signal contrast in high resolution 2D and 3D functional activation imaging of the motor cortex at 1.5 T: preliminary results. *Magn. Reson. Med.* **30**, 387-402 (1993).
23. R. Turner, P. Jezzard, D. Le Bihan, A. Prinster, Contrast mechanisms and vessel size effects in BOLD contrast functional neuroimaging, in "Proc., SMRM, 12th Annual Meeting, 1993," p. 173.
24. C. T. W. Moonen, G. Liu, P. van Gelderen, G. Sobering, A fast gradient-recalled MRI technique with increased sensitivity to dynamic susceptibility effects. *Magn. Reson. Med.* **26**, 184-189 (1992).
25. G. Liu, G. Sobering, A. W. Olson, P. van Gelderen, C. T. W. Moonen, Fast echo-shifted gradient-recalled MRI: combining a short repetition time with variable T_2^* weighting. *Magn. Reson. Med.* **30**, 68-75 (1993).
26. C. T. W. Moonen, F. Barrios, J. R. Zigun, J. Gillen, G. Liu, G. Sobering, R. Sexton, J. Woo, J. Frank, D. R. Weinberger, Functional brain MR imaging based on bolus tracking with a fast T_2^* sensitized gradient-echo method. *Magn. Reson. Imaging* **12**, 379-385 (1994).
27. J. H. Duyn, C. T. W. Moonen, V. S. Mattay, R. H. Sexton, F. A. Barrios, G. S. Sobering, J. A. Frank, G. Liu, D. R. Weinberger, 3-Dimensional functional imaging of human brain using echo-shifted FLASH, in "Proc., SMRM, 12th Annual Meeting, 1993," p. 1386.
28. G. Sobering, F. Barrios, C. T. W. Moonen, D. R. Weinberger, J. Frank, V. S. Mattay, R. S. Sexton, Auto-correlation analysis of functional MRI, in "Proc., SMRM, 12th Annual Meeting, 1993," p. 449.
29. P. A. Bandettini, A. Jesmanowicz, E. C. Wong, J. S. Hyde, Processing strategies for time-course data sets in functional MRI of the human brain. *Magn. Reson. Med.* **30**, 161-173 (1993).
30. J. R. Zigun, J. A. Frank, F. A. Barrios, D. W. Jones, T. K. F. Foo, C. T. W. Moonen, D. Z. Press, D. R. Weinberger, Measurement of brain activity with bolus administration of contrast agent and gradient-echo MR imaging. *Radiology* **186**, 353-356 (1993).